Mitochondria–A target for attenuation of astrocyte pathology

Morch, Marlene Thorsen; Khorooshi, Reza; Marczynska, Joanna; Dubik, Magdalena; Nielsen, Soeren; Nieland, John Dirk; Asgari, Nasrin; Owens, Trevor

Published in:
Journal of Neuroimmunology

DOI:
10.1016/j.jneuroim.2021.577657

Publication date:
2021

Document version:
Final published version

Journal of Neuroimmunology 358 (2021) 577657

Contents lists available at ScienceDirect

Journal of Neuroimmunology

journal homepage: www.elsevier.com/locate/jneuroim

Short Communication

Mitochondria–A target for attenuation of astrocyte pathology

Marlene Thorsen Morch [a,b], Reza Khorooshi [a,b], Joanna Marczynska [a,b], Magdalena Dubik [a], Soeren Nielsen [c], John Dirk Nieland [c], Nasrin Asgari [a,b,d], Trevor Owens [a,b,*]

[a] Neurobiology Research, Department of Molecular Medicine, University of Southern Denmark, 5000 Odense C, Denmark
[b] BRIDGE, Brain Research - Inter-Disciplinary Guided Excellence, 5000 Odense C, Denmark
[c] Department of Health Science and Technology, Aalborg University, 9220 Aalborg East, Denmark
[d] Department of Neurology, Slagelse Hospital, Institute of Regional Health Research, 4200 Slagelse, Denmark

ARTICLE INFO

Keywords:
Astrocyte pathology
Mitochondrial dysfunction
Central nervous system
Etomoxir
Neuromyelitis optica spectrum disorder
Metabolic

ABSTRACT

Astrocyte pathology is a feature of neuromyelitis optica spectrum disorder (NMOSD) pathology. Recently mitochondrial dysfunction and metabolic changes were suggested to play a role in NMOSD. To elucidate the role of mitochondrial dysfunction, astrocyte pathology was induced in C57BL/6 J female mice by intracerebral injection of aquaporin-4-immunoglobulin G from an NMOSD patient, together with complement. Etomoxir has been shown to cause mitochondrial dysfunction. Etomoxir was delivered to the central nervous system and resulted in decreased astrocyte pathology. The ameliorating effect was associated with increases in different acylcarnitines and amino acids. This suggests that mitochondria may be a therapeutic target in NMOSD.

1. Introduction

The pathological hallmarks of neuromyelitis optica spectrum disorder (NMOSD) include astrocyte pathology, caused by disease-specific autoantibody against the astrocyte water channel aquaporin-4 (AQP4) in the central nervous system (CNS) (Bennett and Owens, 2017; Weinshenker and Wingerchuk, 2017). Recently mitochondrial dysfunction has been suggested to play a role in disease progression, disability level and cognitive impairment (Foolad et al., 2020). Mitochondrial DNA in cerebrospinal fluid was elevated in the acute phase of NMOSD (Yamashita et al., 2018) and associated to disease severity (Peng et al., 2020). Additionally, an altered energy metabolism has been associated to disease (Jurynczyk et al., 2017; Kim et al., 2017). This points to a role for mitochondria in disease development and progression.

The drug etomoxir results in altered metabolism through interaction with mitochondria at different levels. It blocks beta-oxidation by inhibiting the activity of carnitine palmitoyl transferase-1 (CPT-1), an enzyme involved in transport of lipids across the mitochondrial membrane (Bonnefont et al., 2004; Houten and Wanders, 2010), and it inhibits oxidative phosphorylation through actions on complex I in the electron transport chain (O'Connor et al., 2018; Yao et al., 2018). These actions have been shown to induce mitochondrial dysfunction (Vickers et al., 2006). We therefore utilized etomoxir to examine how alterations in metabolism as well as mitochondrial dysfunction influence astrocyte pathology.

2. Methods

2.1. Mice

Young adult (8–12 weeks) female C57Bl/6J mice (Taconic, Lille Skensved, Denmark) were housed in the Biomedical Laboratory, University of Southern Denmark. Experiments were conducted in accordance with the National Ethical Committee, Animal Experiments Inspectorate under the Danish Ministry of Food, Agriculture and Fisheries, and The Danish Veterinary and Food Administration (approval number 2020-15-0201-00652). Use of human material (NMO-IgG) was approved by the Committee on Biomedical Research Ethics for the Region of Southern Denmark (ref. no. S20080142).

Abbreviations: AQP4, aquaporin 4; C, complement; CPT-1, carnitine palmitoyl transferase-1; NMO-IgG, human IgG from neuromyelitis optica spectrum disorder patients positive for AQP4-IgG; Normal-IgG, human IgG from healthy donors.

* Corresponding author at: Neurobiology Research, Department of Molecular Medicine, University of Southern Denmark, 5000 Odense C, Denmark.
E-mail addresses: mmorch@health.sdu.dk (M.T. Morch), rkhorooshi@health.sdu.dk (R. Khorooshi), jmarczynska@health.sdu.dk (J. Marczynska), mdubik@health.sdu.dk (M. Dubik), sn@cpt.one (S. Nielsen), jdn@hst.aau.dk (J.D. Nieland), nasgari@health.sdu.dk (N. Asgari), towens@health.sdu.dk (T. Owens).

https://doi.org/10.1016/j.jneuroim.2021.577657
Received 28 January 2021; Received in revised form 2 July 2021; Accepted 8 July 2021
Available online 14 July 2021

2.2. Induction of astrocyte pathology and treatment

Mice were anesthetized by isoflurane inhalation or subcutaneous injection of a mixture of 0.79 μg Fentanylcitrate, 25 μg Fluanisone, 1,25 μg methylparahydroxybenzoate and 12.5 μg midazolam in water / 10 g body weight. We observed no differences or grouping in the calculated loss of AQP4 or GFAP with regards to anaesthesia protocol, therefore we conclude that anaesthesia protocols did not affect outcome. Stereotactic coordinates were relative to bregma: 2 mm lateral, 0.2 mm anterior and 3.5 mm ventral. A 30-gauge needle attached to a 50 μl Hamilton syringe was inserted and a total of 6 μl was infused at 1 μl/min (150 μg NMO-IgG (patient-derived) or normal-IgG (healthy donor) + 144 μg complement (C) (healthy donors) (Asgari et al., 2013), with or without etomoxir (0.5 μg, Merck, Sigma-Aldrich, Søborg, Denmark)). Two days later mice received a total volume of 10 μl containing etomoxir (0.5 μg, Merck, Sigma-Aldrich) or vehicle (HBSS) intrathecally via cisterna magna. Mice were sacrificed at day 4. Brains were dissected out and processed as previously described (Asgari et al., 2013).

2.3. Immunostaining

Brains were cut on a cryostat into serial coronal sections of 12 μm thickness spanning the lesion and stained with primary antibodies against AQP4 (Alomone Labs Ltd. Jerusalem, Israel, 8 μg/ml), glial fibrillary acidic protein (GFAP) (DAKO, Denmark, 2.9 μg/ml). The sections were incubated with biotinylated goat anti-rabbit IgG (Abcam, 2,5 μg/ml), followed by incubation with streptavidin-horseradish peroxidase (Cytiva, Brønshøj, Denmark) and developed with 3,3′-diaminobenzidine (Merck).

2.4. Quantification of lesions

Images were acquired using an Olympus BX51 microscope with an Olympus DP73 camera (Olympus, Ballerup, Denmark). Loss of AQP4 and GFAP staining was quantified as percentage of the ipsilateral hemisphere. The area of loss was measured and then divided by the area of the ipsilateral hemisphere. Measurements were done using the free software Fiji, ImageJ. Fold change was then attained by calculating the average value for control and then all measured values both for the control group and for the etomoxir group were divided by the control group average. ((measured values)/(average value calculated from control group) = fold change values).

2.5. Measurement of acylcarnitines and animo acids

Approximately 100 mg brain tissue including the lesion were dissected out and collected in 1 ml radioimmunoprecipitation assay (RIPA) lysis and extraction buffer. Samples were homogenized by sonication then spun down at 14000 *g* for 15 min.

The metabolite extraction and butanol derivatization are based on a previously described method (Rashed et al., 1995). All samples were measured in triplicates. Briefly, 5 μL of each sample was added to a well of a 96-well filter plate with semipermeable membrane (Multiscreen-HV, 0.45 μm, Merck, USA). The samples were extracted with 120 μL of methanol containing known concentrations of deuterated labeled amino acid and acylcarnitine standards (Cambridge Isotope Laboratory, UK). The labeled standards had the following concentrations: ^{15}N, 2-^{13}C-Glycine, 12.5 μM; [$^{2}H_4$]-Alanine, 2.5 μM; [$^{2}H_8$]-Valine, 2.5 μM; [$^{2}H_3$]-Leucine, 2.5 μM; [$^{2}H_3$]-Methionine, 2.5 μM; [$^{2}H_5$]-Phenylalanine, 2.5 μM; [$^{2}H_4$]-Tyrosine, 2.5 μM; [$^{2}H_3$]-Aspartate, 2.5 μM; [$^{2}H_3$]-Glutamate, 2.5 μM; [$^{2}H_2$]-Ornithine-2HCl, 2.5 μM; [$^{2}H_2$]-Citrulline, 2.5 μM; [$^{2}H_4$]; 5-^{13}C-Arginine, 2.5 μM; [$^{2}H_9$]-Carnitine, 0.76 μM; [$^{2}H_3$]-Acetylcarnitine, 0.19 μM; [$^{2}H_3$]-Propionylcarnitine, 0.04 μM; [$^{2}H_3$]-Butyrylcarnitine, 0.04 μM; [$^{2}H_9$]-Isovalerylcarnitine, 0.04 μM; [$^{2}H_3$]-Octanoylcarnitine, 0.04 μM; [$^{2}H_9$]-Myristoylcarnitine, 0.04 μM; [$^{2}H_3$]-Palmitoylcarnitine, 0.08 μM. The plates were covered and shaken at room temperature for 45 min on a horizontal shaker. The samples were then filtered into a 96-well polypropylene microplate by centrifugation (3000 rpm for 5 min) and evaporated under air at 55 °C until dry. For the butanol derivatization, 60 μL of n-butanol in HCl was added to each sample well and the plate incubated at 65 °C for 20 min. The samples were evaporated again and reconstituted in 100 μL of acetonitrile/H_2O (80:20).

The concentrations of amino acids and acylcarnitines were measured using flow-injection analysis coupled with tandem mass spectrometry (FIA-MS/MS). The FIA-MS/MS analysis was carried out on a Quattro Micro triple-quadrupole tandem mass spectrometer (Waters, UK) equipped with a liquid chromatography pump and autosampler (Alliance High Throughput HPLC, Waters, UK) operating in positive ionization mode. Acylcarnitines and free carnitine were analyzed by the precursor-ion scan of *m/z* 85; amino acids were analyzed by two scan functions, the neutral amino acids with neutral loss of m/z 102 and basic amino acids with neutral loss of m/z 119. Lastly, glycine, arginine, and argininosuccinic acid and their corresponding internal standards were analyzed in multiple reaction monitoring (MRM) mode.

2.6. Statistical analysis

Statistical analysis was done using GraphPad Prism version 9 (GraphPad Software Inc., San Diego, CA, USA). Data were examined for outliers using the ROUT test (Q = 1) and identified outliers were excluded from further testing. Significant differences were calculated using multiple or single Mann–Whitney test, assuming a nonparametric distribution. Data are presented as mean ± SEM. Values of $p < 0.05$ are considered statistically significant.

3. Results

To ascertain metabolic effect in our model of astrocyte pathology, etomoxir was co-injected intrastriatally with normal-IgG + C or NMO-IgG + C to C57BL/6 mice on day zero and intrathecally injected on day two. Mice were sacrificed four days post intra-striatal injection and lesion and surrounding tissue were analyzed by FIA-MS/MS. Surprisingly, administration of etomoxir resulted in increased levels of short (C3DC, C5-OH), medium (C8:1, C8DC, C10DC, C12DC), long (C16:1-OH) and very long (C22, C26) chain acylcarnitines (Fig. 1A) and some amino acids (glutamine, lysine and valine) (Fig. 1B). However, levels of tyrosine were decreased (Fig. 1B). We next examined if the changes induced by etomoxir were associated to changes in development of astrocyte pathology. We have previously shown that injection of normal-IgG + C and NMO-IgG alone did not cause loss of AQP4 or GFAP (Asgari et al., 2013; Khorooshi et al., 2013; Mørch et al., 2018; Wlodarczyk et al., 2020). NMO-IgG + C induced lesions of astrocyte pathology, identified by loss of AQP4 and GFAP (Fig. 2A, the area with pathology is outlined) as well as deposition of complement and human IgG (not shown). Unexpectedly, administration of etomoxir directly in the CNS visibly reduced astrocyte pathology (loss of AQP4 and GFAP) (Fig. 2B), and significantly reduced the quantification of both loss of AQP4 (Fig. 2C) and GFAP (Fig. 2D). Histological analysis of microglia using Iba1 staining showed no visual change in activation by etomoxir (supp. Fig. S1).

4. Discussion

This study examined the effect of mitochondrial dysfunction in the CNS on astrocyte pathology. Local treatment with etomoxir in the CNS was associated with increased acylcarnitines and amino acids and surprisingly, reduced astrocyte pathology.

As far as we are aware, this is the first study of the role of etomoxir directly in the CNS as well as being the first study on the role of mitochondria in NMO-IgG induced astrocyte pathology. Etomoxir has previously been shown to ameliorate CNS pathology in experimental

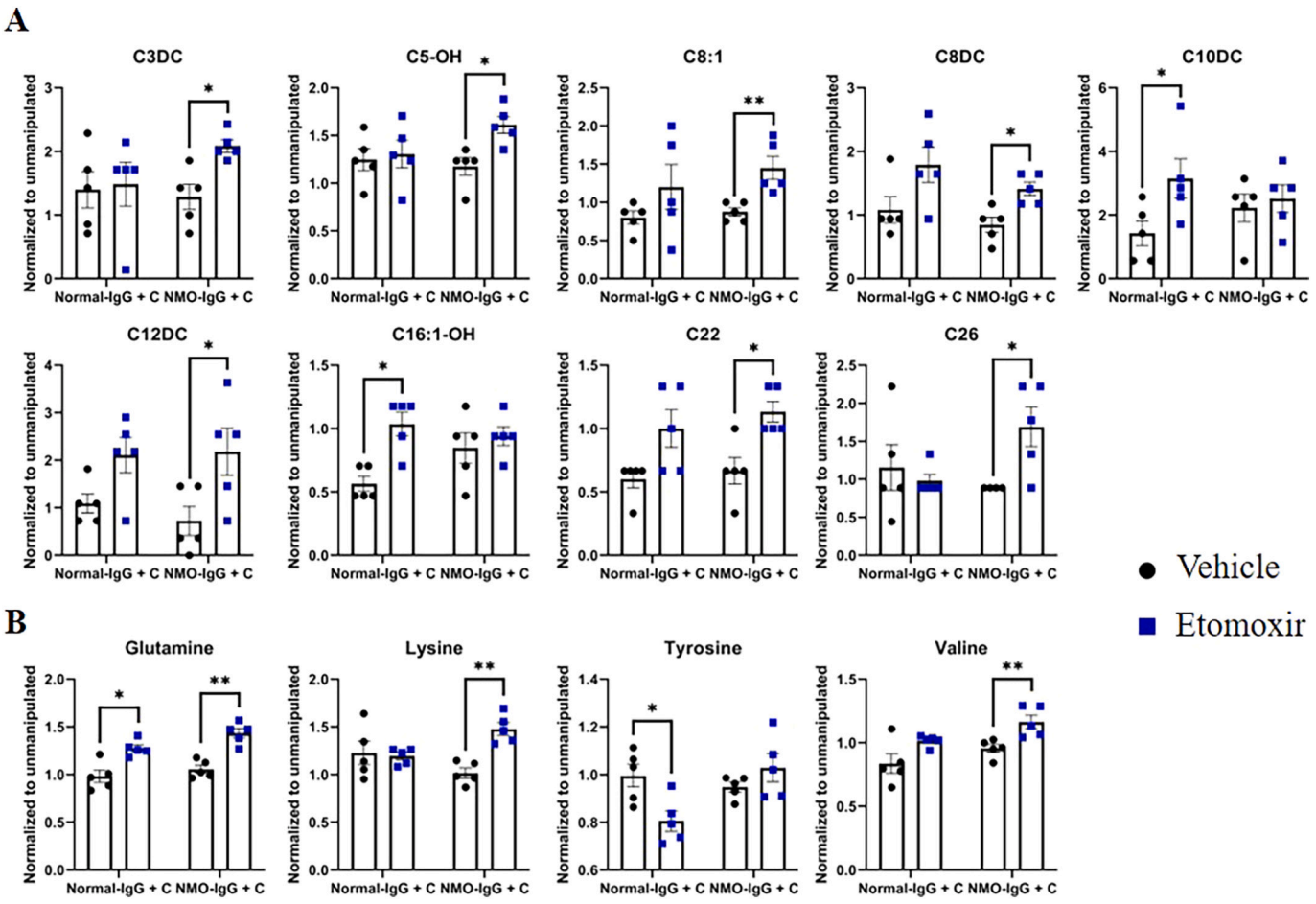

Fig. 1. Etomoxir affects acylcarnitines in the CNS parenchyma.
C57BL/6 J female mice were injected with Normal-IgG + C or NMO-IgG + C to striatum. The mice were treated with vehicle or etomoxir on day 0 (intracerebral) and again on day two (intrathecal). Mice were sacrificed on day four. A tissue block of approximately 100 mg containing the lesioned area was microdissected out and acylcarnitines and amino acids were measured using flow-injection analysis coupled with tandem mass spectrometry in both the vehicle and etomoxir group (fold change to vehicle, $n = 5$). A: Acylcarnitines with significant changes after treatment with etomoxir in either Normal-IgG + C or NMO-IgG + C group. B: Significant changes in amino acids after etomoxir treatment in either Normal-IgG + C or NMO-IgG + C group.
Outliers were identified using the ROUT test, Q = 1, then removed. Nonparametric Mann-Whitney *U* test was used for statistical analysis. $^{*}P \leq 0.05$ and $^{**}P \leq 0.01$. Results are presented as mean ± SEM.

autoimmune encephalomyelitis (Shriver and Manchester, 2011; Mørkholt et al., 2018). However, the treatment was administered peripherally, and it cannot be excluded that the ameliorating effect of etomoxir was due to effects on the peripheral lymphoid compartment - etomoxir treatment of T cell cultures resulted in reduced interferon-gamma levels and increased apoptosis (Shriver and Manchester, 2011). In the current study we utilized a model that mimics the astrocyte pathology seen in NMOSD. NMO-IgG + C is administered directly to the CNS with minimal involvement of the peripheral immune compartment. This would support that the effect of etomoxir which we observed was a direct CNS effect.

Mitochondrial dysfunction has been implicated in motor and cognitive symptoms of NMOSD (Foolad et al., 2020), and CSF correlates were associated to development of pathology (Yamashita et al., 2018; Peng et al., 2020). Unexpectedly, we observed here that changes in mitochondrial function caused by etomoxir resulted in amelioration of astrocyte pathology. Astrocytes themselves may have been directly affected by etomoxir. Although astrocytes with dysfunctional mitochondria survive and do not cause glial pathology (Supplie et al., 2017), functional mitochondrial electron transport chain and oxidative phosphorylation machinery in astrocytes were required for neuroprotection in a model for ischemic stroke (Fiebig et al., 2019). In the current study we found no obvious evidence of astrocyte reactivity having been affected by etomoxir. Another question is whether pathology and its protection should necessarily reflect mitochondrial dysfunction in astrocytes. We have previously shown that microglia play a central role in development of NMOSD-like pathology in our model, as depletion of microglia resulted in reduced astrocyte pathology (Wlodarczyk et al., 2020). Anti-inflammatory microglia/macrophages rely on oxidative phosphorylation and at times fatty acid oxidation while pro-inflammatory microglia and macrophages undergo a switch towards glycolysis to meet cellular demands and cell survival (Harry et al., 2020). Furthermore, etomoxir has been shown to induce mitochondrial dysfunction (Vickers et al., 2006) and mitochondrial status has been linked to functional outputs eg phagocytosis in macrophages (Chen et al., 2018; Belchamber et al., 2019) and microglia (Rubio-Araiz et al., 2018). Interfering with this shift should reverse inflammation. This could account for the effect of Etomoxir in our study. However, a histological examination of microglia/macrophages reactivity using Iba1 staining showed no immediate differences in activation such as we previously observed in IFNAR1 KO mice (Khorooshi et al., 2013). In the current study, we have demonstrated "proof-of-concept" and we identified a role for mitochondrial function in NMOSD. We report amelioration of NMOSD-like pathology by etomoxir; however, further in-depth studies are needed to clarify dose-response as well as the precise mechanism.

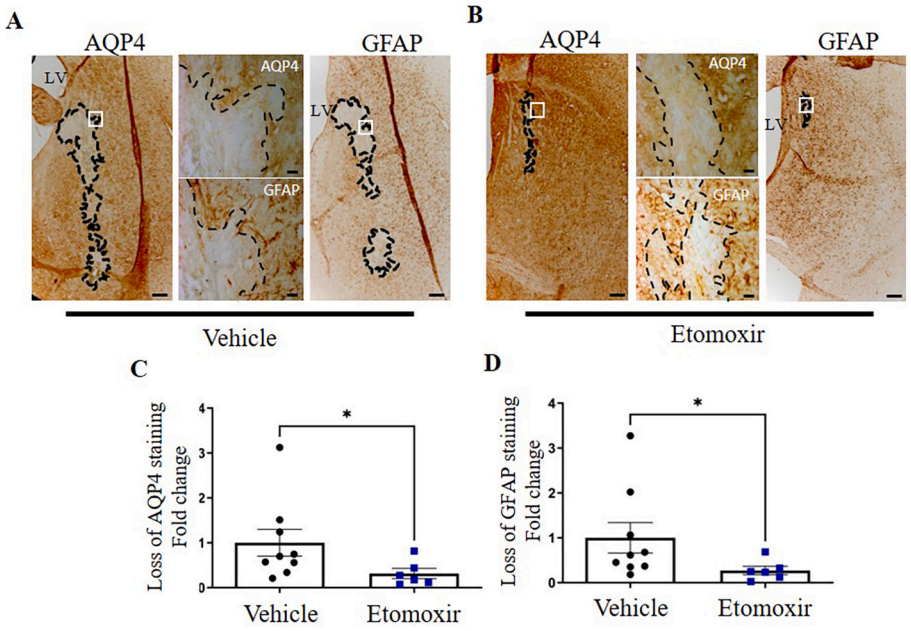

Fig. 2. Etomoxir attenuates AQP4-IgG + C induced astrocyte pathology.
Astrocyte pathology was induced in C57BL/6 J female mice by injection of AQP4-IgG + C to striatum. The mice were treated with vehicle or etomoxir on day 0 (intracerebral) and again on day two (intrathecal). Mice were sacrificed on day four. (A, B): Overview of brain sections from vehicle- and etomoxir-treated mice stained for AQP4 and GFAP. The area with pathology is outlined. (C, D): Bar graphs show the normalized values of AQP4 and GFAP loss from vehicle ($n = 9$) and etomoxir treated ($n = 6$) group.
Outliers were identified using the ROUT test, Q = 1, then removed. Nonparametric Mann-Whitney U test was used for statistical analysis. LV: lateral ventricle. Scale bars for A and B = 200 μm. $^*P \leq 0.05$. Results are presented as mean ± SEM.

Supplementary data to this article can be found online at https://doi.org/10.1016/j.jneuroim.2021.577657.

Data availability statement

The FIA-MS/MS dataset generated for this study can be found in Supplementary Table 1.

Author contributions

MTM wrote the manuscript, performed intrathecal treatment, daily monitoring of mice, histological and statistical analysis, and was involved in study design and development. MTM and RK performed stereotactic injection. JM and MD prepared samples for LC-tandem MS and MTM and JM analyzed the data. TO, NA and RK gave supervision on the design of the study and helped to draft the manuscript. JDN and SN helped develop the study design. All authors reviewed the manuscript.

Funding

This research was supported by the Danish Multiple Sclerosis Society; The Lundbeck Foundation (# R198-2015-171); Ph.D. stipends from The University of Southern Denmark, Health Sciences Faculty; Warwara Larsens Fond; Bjarne Jensens Fond; Augustinus Foundation; Lægefonden; Dagmar Marshalls Fond and Familien Hede Nielsens Fond.

Declaration of Competing Interest

The authors declare that the research was conducted in the absence of any commercial or financial relationships that could be construed as a potential conflict of interest.

Acknowledgments

We thank Dina S. Arengoth and Pia Nyborg Nielsen for advice on animal handling and operating procedures and technical support, respectively. We thank Søren Lillevang (Clinical Immunology Department, Odense University Hospital) and Lars Vitved (Department of Cancer and Inflammation Research, IMM, SDU) for antibody characterization and purification. We thank Leifur Franzson, Sheilah Severino and Freyr Jóhannsson (Department of Genetics and Molecular Medicine, Landspitali, Iceland) for preforming FIA-MS/MS and analyzing those data.

References

Asgari, N., Khorooshi, R., Lillevang, S.T., Owens, T., 2013. Complement-dependent pathogenicity of brain-specific antibodies in cerebrospinal fluid. J. Neuroimmunol. 254, 76–82. https://doi.org/10.1016/j.jneuroim.2012.09.010.

Belchamber, K.B.R., Singh, R., Batista, C.M., Whyte, M.K., Dockrell, D.H., Kilty, I., et al., 2019. Defective bacterial phagocytosis is associated with dysfunctional mitochondria in COPD macrophages. Eur. Respir. J. 54. https://doi.org/10.1183/13993003.02244-2018.

Bennett, J.L., Owens, G.P., 2017. Neuromyelitis optica: deciphering a complex immune-mediated Astrocytopathy. J. Neuroophthalmol. 37, 291–299. https://doi.org/10.1097/WNO.0000000000000508.

Bonnefont, J.-P., Djouadi, F., Prip-Buus, C., Gobin, S., Munnich, A., Bastin, J., 2004. Carnitine palmitoyltransferases 1 and 2: biochemical, molecular and medical aspects. Mol. Asp. Med. 25, 495–520. https://doi.org/10.1016/j.mam.2004.06.004.

Chen, Q., Wang, N., Zhu, M., Lu, J., Zhong, H., Xue, X., et al., 2018. TiO2 nanoparticles cause mitochondrial dysfunction, activate inflammatory responses, and attenuate phagocytosis in macrophages: a proteomic and metabolomic insight. Redox Biol. 15, 266–276. https://doi.org/10.1016/j.redox.2017.12.011.

Fiebig, C., Keiner, S., Ebert, B., Schäffner, I., Jagasia, R., Lie, D.C., et al., 2019. Mitochondrial dysfunction in astrocytes impairs the generation of reactive astrocytes and enhances neuronal cell death in the cortex upon Photothrombotic lesion. Front. Mol. Neurosci. 12, 40. https://doi.org/10.3389/fnmol.2019.00040.

Foolad, F., Khodagholi, F., Nabavi, S.M., Javan, M., 2020. Changes in mitochondrial function in patients with neuromyelitis optica; correlations with motor and cognitive disabilities. PLoS One 15, e0230691. https://doi.org/10.1371/journal.pone.0230691.

Harry, G.J., Childers, G., Giridharan, S., Hernandes, I.L., 2020. An association between mitochondria and microglia effector function: what do we think we know? Neuroimmunol. Neuroinflam. 7, 150–165. https://doi.org/10.20517/2347-8659.2020.07.

Houten, S.M., Wanders, R.J.A., 2010. A general introduction to the biochemistry of mitochondrial fatty acid β-oxidation. J. Inherit. Metab. Dis. 33, 469–477. https://doi.org/10.1007/s10545-010-9061-2.

Jurynczyk, M., Probert, F., Yeo, T., Tackley, G., Claridge, T.D.W., Cavey, A., et al., 2017. Metabolomics reveals distinct, antibody-independent, molecular signatures of MS, AQP4-antibody and MOG-antibody disease. Acta Neuropathol. Commun 5. https://doi.org/10.1186/s40478-017-0495-8.

Khorooshi, R., Wlodarczyk, A., Asgari, N., Owens, T., 2013. Neuromyelitis optica-like pathology is dependent on type I interferon response. Exp. Neurol. 247, 744–747. https://doi.org/10.1016/j.expneurol.2013.02.005.

Kim, H.-H., Jeong, I.H., Hyun, J.-S., Kong, B.S., Kim, H.J., Park, S.J., 2017. Metabolomic profiling of CSF in multiple sclerosis and neuromyelitis optica spectrum disorder by nuclear magnetic resonance. PLoS One 12. https://doi.org/10.1371/journal.pone.0181758.

Mørch, M.T., Sørensen, S.F., Khorooshi, R., Asgari, N., Owens, T., 2018. Selective localization of IgG from cerebrospinal fluid to brain parenchyma. J. Neuroinflammation 15. https://doi.org/10.1186/s12974-018-1159-8.

Mørkholt, A.S., Kastaniegaard, K., Trabjerg, M.S., Gopalasingam, G., Niganze, W., Larsen, A., et al., 2018. Identification of brain antigens recognized by autoantibodies in experimental autoimmune encephalomyelitis-induced animals treated with etomoxir or interferon-β. Sci. Rep. 8. https://doi.org/10.1038/s41598-018-25391-y.

O'Connor, R.S., Guo, L., Ghassemi, S., Snyder, N.W., Worth, A.J., Weng, L., et al., 2018. The CPT1a inhibitor, etomoxir induces severe oxidative stress at commonly used concentrations. Sci. Rep. 8, 6289. https://doi.org/10.1038/s41598-018-24676-6.

Peng, Y., Chen, J., Dai, Y., Jiang, Y., Qiu, W., Gu, Y., et al., 2020. NLRP3 level in cerebrospinal fluid of patients with neuromyelitis optica spectrum disorders: increased levels and association with disease severity. Mult. Scleros. Rel. Disord. 39, 101888. https://doi.org/10.1016/j.msard.2019.101888.

Rashed, M.S., Ozand, P.T., Bucknall, M.P., Little, D., 1995. Diagnosis of inborn errors of metabolism from blood spots by acylcarnitines and amino acids profiling using automated electrospray tandem mass spectrometry. Pediatr. Res. 38, 324–331. https://doi.org/10.1203/00006450-199509000-00009.

Rubio-Araiz, A., Finucane, O.M., Keogh, S., Lynch, M.A., 2018. Anti-TLR2 antibody triggers oxidative phosphorylation in microglia and increases phagocytosis of β-amyloid. J. Neuroinflammation 15, 247. https://doi.org/10.1186/s12974-018-1281-7.

Shriver, L.P., Manchester, M., 2011. Inhibition of fatty acid metabolism ameliorates disease activity in an animal model of multiple sclerosis. Sci. Rep. 1 https://doi.org/10.1038/srep00079.

Supplie, L.M., Düking, T., Campbell, G., Diaz, F., Moraes, C.T., Götz, M., et al., 2017. Respiration-deficient astrocytes survive as glycolytic cells in vivo. J. Neurosci. 37, 4231–4242. https://doi.org/10.1523/JNEUROSCI.0756-16.2017.

Vickers, A.E.M., Bentley, P., Fisher, R.L., 2006. Consequences of mitochondrial injury induced by pharmaceutical fatty acid oxidation inhibitors is characterized in human and rat liver slices. Toxicol. in Vitro 20, 1173–1182. https://doi.org/10.1016/j.tiv.2006.01.021.

Weinshenker, B.G., Wingerchuk, D.M., 2017. Neuromyelitis spectrum disorders. Mayo Clin. Proc. 92, 663–679. https://doi.org/10.1016/j.mayocp.2016.12.014.

Wlodarczyk, A., Khorooshi, R., Marczynska, J., Holtman, I.R., Burton, M., Jensen, K.N., et al., 2020. Type I interferon-activated microglia are critical for neuromyelitis optica pathology. Glia. https://doi.org/10.1002/glia.23938.

Yamashita, K., Kinoshita, M., Miyamoto, K., Namba, A., Shimizu, M., Koda, T., et al., 2018. Cerebrospinal fluid mitochondrial DNA in neuromyelitis optica spectrum disorder. J. Neuroinflammation 15. https://doi.org/10.1186/s12974-018-1162-0.

Yao, C.-H., Liu, G.-Y., Wang, R., Moon, S.H., Gross, R.W., Patti, G.J., 2018. Identifying off-target effects of etomoxir reveals that carnitine palmitoyltransferase I is essential for cancer cell proliferation independent of β-oxidation. PLoS Biol. 16 https://doi.org/10.1371/journal.pbio.2003782.